Integrals of motion and semipermeable surfaces to bound the amplitude of a plasma instability

S. Neukirch*
Centre for Nonlinear Dynamics and its Applications, University College London, Gower Street, London WC1E 6BT, United Kingdom
(Received 24 July 2000; published 15 February 2001)

We study a dissipative dynamical system that models a parametric instability in a plasma. This instability is due to the interaction of a whistler with the ion acoustic wave and a plasma oscillation near the lower hybrid resonance. The amplitude of these three oscillations obey a three-dimensional system of ordinary differential equations which exhibits chaos for certain parameter values. By using certain ''integrability informations'' we have on the system, we get geometrical bounds for its chaotic attractor, leading to an upper bound for its Lyapunov dimension. On the other hand, we also obtain ranges of values of the system's parameters for which there is no chaotic motion.

DOI: 10.1103/PhysRevE.63.036202 PACS number(s): 05.45.Ac, 02.30.Hq, 52.35.Py

I. INTRODUCTION

A whistler is a wave in a plasma which propagates parallel to the magnetic field. It is produced by currents outside the plasma at a frequency less than that of the electron cyclotron frequency. Also it is circulary polarized, rotating about the magnetic field in the same sense as the electrons in the plasma.

Interactions between these whistler waves and lower hybrid waves in a plasma are among the important phenomena taking place in the ionosphere [1]. As it has been shown in [2], a whistler can destabilize a magnetoactive plasma by exciting the lower hybrid wave together with the ion acoustic wave (the longitudinal compression wave in the ion density of a plasma). This parametric excitation, although restrained by the loss of energy which is given to the other nonresonant waves, may become chaotic for certain ranges of value of the pump amplitude. More specifically, the whistler at frequency ω_q excites a plasma wave at frequency ω_k and the ion acoustic wave at frequency $\Omega_\chi=\omega_q-\omega_k$. We call a_k the normal amplitude of the wave at frequency ω_k and b_χ the normal amplitude of the ion acoustic wave. As a result of the decay of these excitations, at least a third synchronous wave is produced (of normal amplitude a_{k_1}) which is linearly damped and will act as a limiter for the instability. This elementary limiting process may nevertheless induce complicated oscillations of the three waves when the pump amplitude is increased.

The differential equations for the amplitudes of the three waves are obtained from the hydrodynamic equation for the radio-frequency oscillation of an electron gas and from the kinetic equation for the ion acoustic wave. The amplitudes are assumed to be constant in space. The evolution equations take the dimensionless form:

$$\dot{a}_k=-b_\chi a_{k_1}-\nu_1 a_k+hb_\chi^\star,$$

$$\dot{b}_\chi=a_k a_{k_1}^\star-\nu_2 b_\chi+ha_k^\star, \tag{1}$$

$$\dot{a}_{k_1}=a_k b_\chi^\star-a_{k_1},$$

where the amplitudes have been nondimensionalized; h is proportional to the amplitude of the electric field of the whistler and ν_1 and ν_2 are the damping decrements of the excited hybrid and acoustic waves normalized to the damping of the decay-induced (third) wave: $\nu_1=\gamma_k/\gamma_{k_1}$, $\nu_2=\gamma_x/\gamma_{k_1}$. Depending on the relative values of h compared to (ν_1,ν_2), the system can relax to trivial equilibrium (no oscillation) or stabilize on a steady oscillation or even present chaotic motion. By studying the dynamics of the phases of a_k, b_χ, and a_{k_1} it can be shown [2] that they correlate as $t\to+\infty$. Hence we shall study system (1) with real amplitudes.

II. THE DYNAMICS AND ROUTE TO CHAOS OF THE PIKOVSKII-RABINOVITCH-TRAKHTENGERTS SYSTEM

We set $x=a_k$, $y=b_\chi$, and $z=a_{k_1}$ and $x,y,z\in\mathbb{R}^3$ and rewrite system (1) as

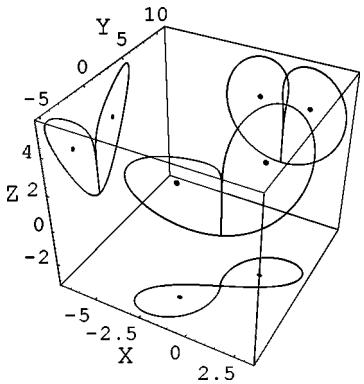

FIG. 1. Double homoclinic trajectory for system (2) with $\nu_1=1$, $\nu_2=4$, $\nu_3=1$, and $h\simeq 3.99$. The trajectory and three projections are drawn. For only slightly greater values of h the system exhibits transient chaotic dynamics. Note that the homoclinic trajectory heads back toward the origin by positive z (tangent to the z axis).

*Electronic address: s.neukirch@ucl.ac.uk

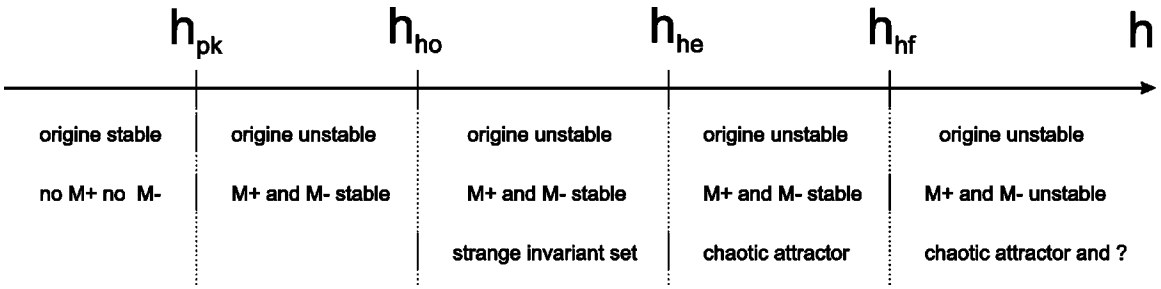

FIG. 2. Schematic route to chaos for the system (2). With $\nu_1=1$, $\nu_2=4$, and $\nu_3=1$, we have $h_{\rm pk}=2$, $h_{\rm hf}\simeq 5$, $h_{\rm he}\simeq 4.8$, and $h_{\rm ho}\simeq 3.99$. As we shall see, for some other values of ν_1 and ν_2, $h_{\rm ho}$ does not exist.

$$(\dot{x},\dot{y},\dot{z})^T=\boldsymbol{F}(x,y,z)=(hy-\nu_1 x-yz,hx-\nu_2 y+xz,xy-\nu_3 z)^T. \quad (2)$$

We will refer at this system as the Pikovskii-Rabinovitch-Trakhtengerts (PRT) system as it has been introduced in [2]. The system is symmetrical about the transformation: $x\rightarrow -x, y\rightarrow -y$. The four parameters are assumed to be positive. We will briefly recall its important features. The origin $O(0,0,0)$ is asymptotically stable for $h<h_{\rm pk}=\sqrt{\nu_1\nu_2}$. At $h=h_{\rm pk}$, two stable equilibrium points

$$M_{\pm}\left(\pm\sqrt{\frac{\nu_3}{\nu_1}z_0(h-z_0)},\pm\sqrt{\nu_1\nu_3\frac{z_0}{h-z_0}},z_0=\sqrt{h^2-\nu_1\nu_2}\right)$$

appear in a pitchfork bifurcation, as the origin loses its stability.

If one increases h further, different bifurcations occur as the motion in phase space becomes more and more complicated (see Fig. 1):

At $h=h_{\rm ho}$ a homoclinic bifurcation takes place: the one-dimensional (1D) unstable manifold of the origin (tangent to the $z=0$ plane) becomes connected with its 2D stable manifold (see Fig. 2). Note that in this figure, the homoclinic trajectory heads back toward the origin through positive z and tangent to the z axis. Considering the orientation of the two stable eigenvectors and the respective values of the two real negative eigenvalues, the finishing part of the homoclinic orbit (if there is one) will lie in the $z=0$ plane for $h<\sqrt{(\nu_3-\nu_1)(\nu_3-\nu_2)}$ and $\nu_3>\nu_1$ and $\nu_3>\nu_2$ and will be tangent to the z axis otherwise. In this latter case it could well be that the homoclinic orbit reaches back to the origin by negative z, but in numerical experiments, following the orbit while changing parameters, we only saw a configuration like in Fig. 2 (tangency to z axis, positive z) and we conjecture that it is always the case. We believe that this bifurcation plays an important role in the dynamics of the system and that the so-called homoclinic explosions, introduced in the study of the Lorenz system in [3], occur here also.[1] Moreover, we assume that the chaotic motion has its source in this homoclinic bifurcation since at this point, $h=h_{\rm ho}$, a strange invariant set (not stable) is born.

This set becomes stable at $h=h_{\rm he}$ when the heteroclinic bifurcation takes place: the left (respectively right) part of the 1D unstable manifold of the origin becomes connected with the 1D stable manifold of the limit cycle (of saddle type) surrounding the equilibrium point M_+ (respectively M_-) (see Fig. 3). Note that up to now, the points $M\pm$ are still stable, so we have three competiting attractors in the phase space.

The $M_\pm$ points lose their stability in a subcritical Hopf bifurcation at $h=h_{\rm hf}$.

The values of $h_{\rm ho}$, $h_{\rm he}$, and $h_{\rm hf}$ depend on ν_1, ν_2, and ν_3, and this defines hypersurfaces in the 4D parameter space. The Hopf bifurcation equation defining $h_{\rm hf}$ is

$$4\nu_1^2\nu_2^2+h^2[(\nu_1-\nu_2)^2+(\nu_1+\nu_2)\nu_3]+h(\nu_1-\nu_2)\times(\nu_3+\nu_1+\nu_2)\sqrt{h^2-\nu_1\nu_2}=0 \quad (\text{with } \nu_2>\nu_1+\nu_3). \quad (3)$$

As for the homoclinic $[h=h_{\rm ho}(\nu_1,\nu_2,\nu_3)]$ and the heteroclinic $[h=h_{\rm he}(\nu_1,\nu_2,\nu_3)]$ bifurcation curves, we cannot calculate them analytically and so we must approximate them numerically (see Fig. 10). Nevertheless we will introduce algebraic bounds to the homoclinic curve in the parameter

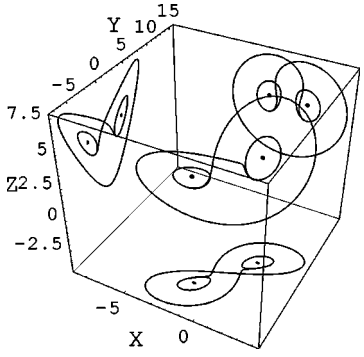

FIG. 3. Double heteroclinic trajectory for system (2) with $\nu_1=1$, $\nu_2=4$, $\nu_3=1$, and $h\simeq 4.8$. We have drawn three projections of the trajectory as well. For greater values of h, the system exhibits stable chaotic dynamics.

[1]In fact, the chaotic attractor of the PRT system (2) and the Lorenz attractor look similar. So do the routes to chaos of these two systems. Nevertheless, the PRT system has one more nonlinearity and is more symmetric in $x\leftrightarrow y$.

space. For $\nu_1=1$, $\nu_2=4$, and $\nu_3=1$, we have $h_{pk}=2$ and $h_{hf}\simeq 5$. Thanks to numerical integration, we find $h_{he}\simeq 4.8$ and $h_{ho}\simeq 3.99$.

III. INTEGRALS OF MOTION AND SEMIPERMEABLE SURFACES

We now turn to the ''integrability information'' we have on system (2). We will show how to use this information to study the chaotic features of the system. There are seven known integrals of motion for system [4]:

1. $I_1=(x^2+y^2-4hz)e^{2\nu t}$ when $\nu=\nu_1=\nu_2=\nu_3/2$.
2. $I_2=(x^2-y^2+2z^2)e^{2\nu t}$ when $\nu_1=\nu_2=\nu_3=\nu$.
3. $I_3=(x^2+y^2)e^{2\nu t}$ when $h=0,\nu_1=\nu_2=\nu$.
4. $I_4=y^2-(z+h)^2$ when $\nu_2=\nu_3=0$.
5. $I_5=x^2+(z-h)^2$ when $\nu_1=\nu_3=0$.
6. $I_6=(y^2+z^2)e^{2\nu t}$ when $\nu_2=\nu_3=\nu$ and $h=0$.
7. $I_7=(x^2-z^2)e^{2\nu t}$ when $\nu_1=\nu_3=\nu$ and $h=0$.

Integrals of motion of higher degree have been searched for, but none were found [4]. Thanks to a rescaling,[2] we can set $\nu_3=1$ [in fact there was no ν_3 in system (1), it has been introduced to enable to existence of I_4 and I_5]. In [5] it has been shown that the existence of an integral of motion for a certain value of the parameters generally comes together with the existence of transverse sections that exist for a much wider range of the parameters. These transverse sections, also called semipermeable surfaces (in a 3D phase space they are surfaces, crossed in one way by the trajectories), yield important exact information about the asymptotic behavior of the system.

Hence the existence of the integral I_1 when $\nu_1=\nu_2=\frac{1}{2}$ leads us to seek semipermeable surfaces with the following algebraic form:

$$R_1(x,y,z)=z-a(x^2+y^2)-b=0. \tag{4}$$

Surfaces R_1 are paraboloids of revolution about the z axis. As explained in [5–7], we compute the scalar product between the normal vector of R_1 and the vector field and we evaluate this scalar product on the surface $R_1=0$:

$$\dot{R}_{1|R_1=0}(x,y)=a(2\nu_2-1)y^2+(1-4ah)xy+a(2\nu_1-1)x^2-b. \tag{5}$$

$\dot{R}_{1|R_1=0}$ is a quadratic polynomial in y, it has constant sign [and hence surfaces (4) are semipermeable] in the three following cases:

(1A) When $\nu_1>\frac{1}{2}$, $\nu_2>\frac{1}{2}$, $h>\sqrt{(\nu_1-\frac{1}{2})(\nu_2-\frac{1}{2})}$, $\forall b\leqslant 0$,

$$0<a_1=\frac{1/4}{h+\sqrt{(\nu_1-\frac{1}{2})(\nu_2-\frac{1}{2})}}$$

[2] $(x,y,z)\to(x,y,z)/\nu_3$, $h\to h/\nu_3$, $t\to t\nu_3$, $\nu_{1,2}\to\nu_{1,2}/\nu_3$.

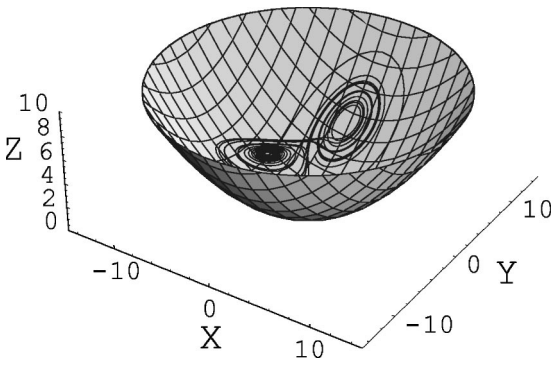

FIG. 4. Chaotic attractor of system (2) bounded by the uppermost semipermeable surface (4) with $b=0$ and $a=a_2$.

$$<a<\frac{1/4}{h-\sqrt{(\nu_1-\frac{1}{2})(\nu_2-\frac{1}{2})}}=a_2.$$

In this case, the chaotic attractor, when it exists, is compelled to evolve above the uppermost surface (4) ($b=0, a=a_2$), see Fig. 4. This case also establishes that, for these values of ν_1, ν_2, and h, all the asymptotic motion (chaotic or not) takes place in the $z>0$ half space.

(1B) $\nu_1>\frac{1}{2}$, $\nu_2>\frac{1}{2}$, $h<\sqrt{(\nu_1-\frac{1}{2})(\nu_2-\frac{1}{2})}<\sqrt{\nu_1\nu_2}$, $\forall b<0$ if $a\in]-\infty;a_2]$ or $\forall b>0$ if $a\in[a_1;+\infty]$. The origin $O(0,0,0)$ is the only equilibrium point in this case, and the semipermeable surfaces (4) establish its asymptotic stability (i.e., all trajectories in phase space eventually stabilize on the origin).

(1C) $\nu_1<\frac{1}{2}$, $\nu_2<\frac{1}{2}$, $\forall(h,b\geqslant 0)$ and $a\in[a_1,a_2]$. The surfaces prevent any homoclinic trajectory from returning to the origin by strictly positive z (see Fig. 5). So for these values of the parameters ν_1 and ν_2 there is no homoclinic bifurcation and hence no chaotic motion $\forall h$.

The existence of integrals of motion I_4 and I_5 lead us to propose

$$R_2(x,y,z)=x^2(\alpha+h)+y^2(\alpha-h)+2h(z-\alpha)^2-\beta. \tag{6}$$

Calculating the scalar product, one finds

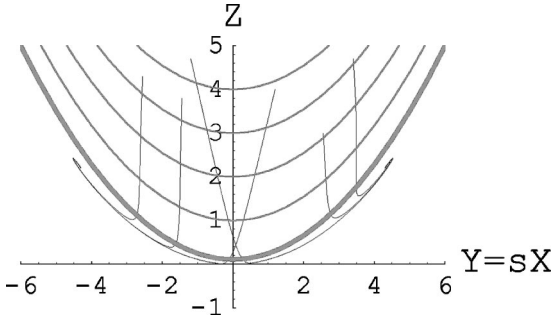

FIG. 5. Semipermeable surfaces (4) prevent the homoclinic bifurcation from taking place when $\nu_1<\frac{1}{2}$, $\nu_2<\frac{1}{2}$, $\forall h$. The coefficient s is chosen in order that the three equilibrium points are on the projection.

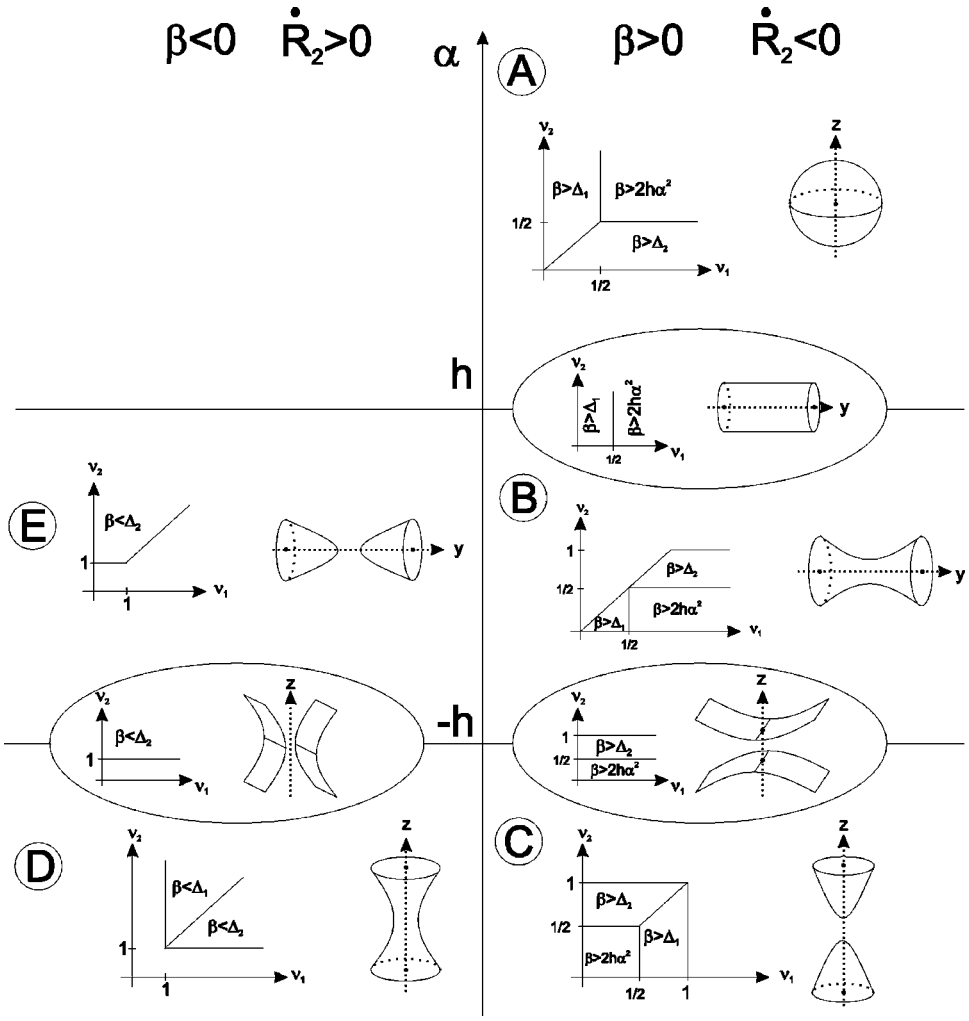

FIG. 6. Shape of surfaces (6) and conditions under which they are semipermeable. $\Delta_i = \alpha^2 h/[2\nu_i(1-\nu_i)]$ with $i=1,2$.

$$\dot{R}_{2|R_2=0}(y,z) = 2hz^2(\nu_1-1) + 2z\alpha h(1-2\nu_1) + y^2(h-\alpha) \times(\nu_2-\nu_1) + \nu_1(2h\alpha^2-\beta) \tag{7}$$

when eliminating the x variable, or

$$\dot{R}_{2|R_2=0}(x,z) = 2hz^2(\nu_2-1) + 2z\alpha h(1-2\nu_2) + x^2(h+\alpha) \times(\nu_2-\nu_1) + \nu_2(2h\alpha^2-\beta) \tag{8}$$

when eliminating the y variable. Depending on α and β, the surfaces (6) can be ellipsoids or hyperboloids of revolution (with y or z axis) with one or two sheets (see Fig. 6).

Case A of Fig. 6 proves that $\forall(h,\nu_1,\nu_2)$ the asymptotic motion is bounded in phase space. The attractor(s) must lie inside the smallest ellipsoid. We have thus to consider the ellipsoid with the smallest radius (β). If we do so, we get something which still depends on α, for example, when $\nu_1 > \frac{1}{2}$ and $\nu_2 > \frac{1}{2}$:

$$\hat{R}_2(x,y,z,\alpha) \overset{\text{def}}{=} R_2(\beta=2h\alpha^2) = x^2(\alpha+h) + y^2(\alpha-h) + 2h(z-\alpha)^2 - 2h\alpha^2 = 0. \tag{9}$$

The center of these semipermeable ellipsoids (9) and their size both depend on α. So one has to consider the envelope of all the ellipsoids (9) when $h<\alpha$, solving

$$\hat{R}_2(x,y,z,\alpha) = 0, \tag{10}$$

$$\frac{d\hat{R}_2}{d\alpha}(x,y,z,\alpha) = 0.$$

One finds

$$E_1: \begin{cases} 4hz = x^2+y^2, \\ x^2+(z-h)^2 = h^2. \end{cases} \tag{11}$$

This corresponds to the inner intersection of a paraboloid and a cylinder. The cylinder is the same as the one we find in case (AB). It establishes that all asymptotic motion for $\nu_1 > \frac{1}{2}$, $\forall(\nu_2,h)$ takes place in the $z>0$ half space. As for the parabola, it does not introduce any improvement to surface (4) with $a=a_2$ and $b=0$.

In case B, the surfaces (6) with $\alpha=0$ show that there can be no homoclinic bifurcation for $\nu_1>\nu_2$ and $\nu_2<1$, $\forall h$ because the 1D unstable manifold of the origin is separated from the 2D stable manifold by the semipermeable surfaces.

Case (BC) shows that there can be no homoclinic bifurcation for $\nu_2<\frac{1}{2}$, $\forall(\nu_1,h)$ for the same reason as in the case (1C).

Case C shows that there can be no homoclinic bifurcation for $\nu_1<\frac{1}{2}$ and $\nu_2<\frac{1}{2}$, $\forall h$ for the same reason as in the previous case.

Case D yields bounds for the chaotic attractor. Here for each ν_1 and ν_2, we have to consider the surface with the smallest β. Then as we still have one free parameter α, we calculate the envelope of the family of surfaces for $\alpha<-h$. This yields

$$E_2=\nu_i(\nu_i-1)(x^2+y^2)[8hz-(x^2+y^2)] +2h^2[(1-2\nu_i)^2(x^2-y^2)+2z^2]=0 \tag{12}$$

with $i=1,2$ and the restriction

$$4hz-(x^2+y^2)<-h^2\frac{(2\nu_i-1)^2}{\nu_i(\nu_i-1)}<0. \tag{13}$$

For points (x,y,z) for which the inequality (13) does not hold, the closest surface from the attractor is the surface (6) with $\alpha=-h$ and $\beta=\Delta_i$. Yet better bounds are found in the next case E where the envelope (12) is to be considered with $i=2$ and for $-h<\alpha<h$ which yields the restrictions

$$-h^2\frac{(2\nu_2-1)^2}{\nu_2(\nu_2-1)}<4hz-(x^2+y^2)\left<h^2\frac{(2\nu_2-1)^2}{\nu_2(\nu_2-1)}\right). \tag{14}$$

The parentheses mean that the upper inequality is of no use because the envelope (12) does not reach $4hz>(x^2+y^2)+h^2(2\nu_2-1)^2/[\nu_2(\nu_2-1)]$. Besides, thanks to surfaces (4), we know that the chaotic attractor lies in the zone where $z>1/4/[h-\sqrt{(\nu_1-\frac{1}{2})(\nu_2-\frac{1}{2})}](x^2+y^2)>(1/4h)(x^2+y^2)>(1/4h)(x^2+y^2)-(h/4)(2\nu_2-1)^2/[\nu_2(\nu_2-1)]$. Hence surface (12) with $i=2$ in case E is a bound for the chaotic attractor with no restriction (see Fig. 7).

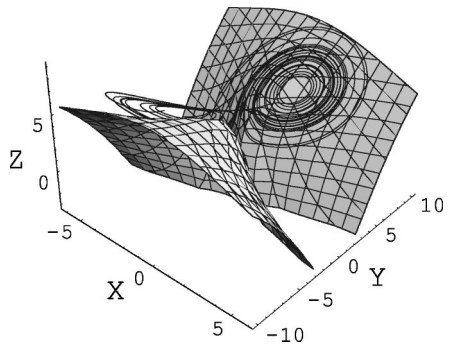

FIG. 7. Chaotic attractor of system (2) with $\nu_1=1$, $\nu_2=4$, $\nu_3=1$, and $h=6$ bounded by the envelope of surfaces (6) in case E defined by Eq. (12) with $i=2$ and $z>0$.

One naturally wonders whether surface (12) is entirely semipermeable or not (and if yes under what conditions). For $\nu_1=\nu_2>1$, we can be sure the answer is yes because in this case surfaces (6) are semipermeable both in cases D and E and so is their envelope. Now if surface (12) is a semipermeable surface, we could wonder if there is an integral of motion (with the same algebraic form) attached to it. Taking $\nu_i=0$ or $\nu_i=1$ in Eq. (12), we find $E_2=2z^2-y^2+x^2$ which corresponds to I_2. And taking $\nu_i=\frac{1}{2}$, we find $E_2=[4hz-(x^2+y^2)]^2$ which corresponds to I_1.

The existence of integrals of motion I_2, I_3, I_6, and I_7 lead us to propose

$$R_3(x,y,z)=x^2A+y^2+(A-1)z^2-B. \tag{15}$$

The scalar product on the surface is

$$\dot{R}_{3|R_3=0}=x^2A(1-\nu_1)+(1-\nu_2)y^2+h(A+1)xy-B. \tag{16}$$

Depending on A and B the surfaces (15) can be ellipsoids or hyperboloids of revolution (with y or z axis) with one or two sheets (see Fig. 8).

$$A_{1\pm}=\frac{-[2h^2+(\nu_1-\nu_2)^2]\pm\sqrt{(\nu_1-\nu_2)^2[4h^2+(\nu_1-\nu_2)^2]}}{2h^2}, \tag{17}$$

$$A_{2\pm}=\frac{-[2h^2-4(\nu_1-1)(\nu_2-1)]\pm4\sqrt{(\nu_1-1)(\nu_2-1)[(\nu_1-1)(\nu_2-1)-h^2]}}{2h^2}, \tag{18}$$

$$A_{3\pm}=\frac{-(2h^2-4\nu_1\nu_2)\pm\sqrt{\nu_1\nu_2-h^2}}{2h^2}. \tag{19}$$

In case F of Fig. 8, the semipermeable ellipsoids state that for these parameter values ($h^2<\nu_1\nu_2$) the origin is asymptotically stable.

Case G is of no interest since here the origin, which is the only equilibrium point, is stable.

Case H provides a bound for the chaotic attractor (see Fig. 9) when $\nu_2>1$ and $\nu_2>\nu_1$.

Case J proves that there is no homoclinic bifurcation (and

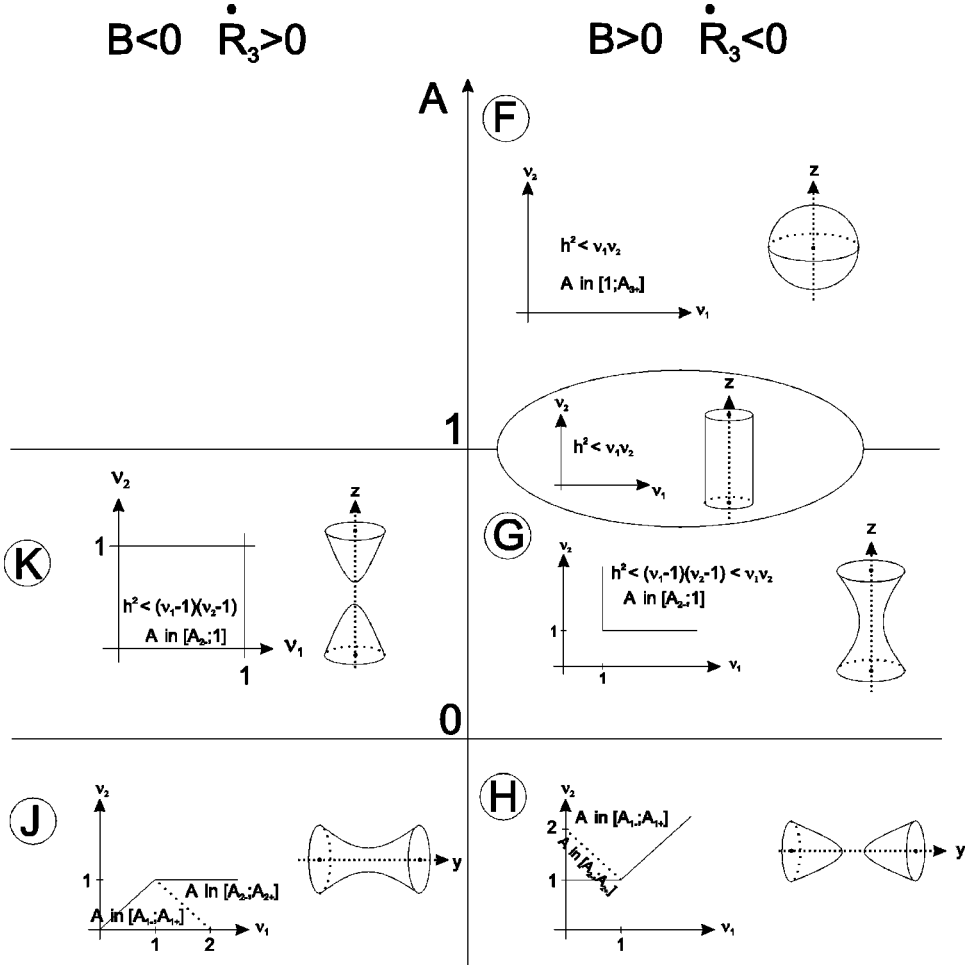

FIG. 8. Shape of the surfaces (15) and conditions for them to be semipermeable. The values of $A_{1\pm}$, $A_{2\pm}$, and $A_{3\pm}$ are given by Eqs. (17), (18), and (19), respectively.

hence no chaotic motion) for $\nu_1 > \nu_2$ and $\nu_2 < 1$ for the same reason as in case B.

In case K, the surfaces (15) are semipermeable when $h < \sqrt{(\nu_1-1)(\nu_2-1)}$ and this prevents the existence of a homoclinic curve tangent to the z axis in its finishing part. But for $h < \sqrt{(\nu_1-1)(\nu_2-1)}$, as we saw earlier, the finishing part of a possible homoclinic curve would not be tangent to the z axis. So this case does not yield any new information.

We have drawn in Fig. 10 the curve $h_{\mathrm{hf}}(\nu_1,\nu_2) = +\infty$ which is the line $\nu_2 = \nu_1 + 1$ [cf. Eq. (3)].

For each (ν_1,ν_2) above this line, there is a value of h for which the equilibrium points $M_\pm$ lose their stability in a subcritical Hopf bifurcation. There are also two different values of h for which the system undergoes homoclinic and heteroclinic bifurcations.

For (ν_1,ν_2) under this line, the equilibrium points $M_\pm$ never lose their stability as h is increased but there may still be values of h for which the homoclinic and heteroclinic bifurcation take place.

Nevertheless we know from surfaces (4), (6), and (15) that for (ν_1,ν_2), the zone where ($\nu_2 < 1$ and $\nu_2 < \nu_1$) or ($\nu_2 < 1/2$), there can be no homoclinic (nor heteroclinic) bifurcation $\forall h$. Hence in between this zone and the line $\nu_2 = \nu_1 + 1$, there must be curves for which $h_{\mathrm{he}} = +\infty$ and $h_{\mathrm{ho}} = +\infty$. We have drawn, thanks to numerical integration, the curves $h_{\mathrm{he}} = 100$ and $h_{\mathrm{ho}} = 100$ which are supposed to be very near the ''∞'' curves. These results on the parameter space drawn in Fig. 10 can be used to understand the different behaviors of the three waves in the plasma. Our method enables us to state that for certain values of the damping decrements ν_1 and ν_2

$$(\nu_2 < 1 \cap \nu_2 < \nu_1) \cup \nu_2 < \tfrac{1}{2}, \tag{20}$$

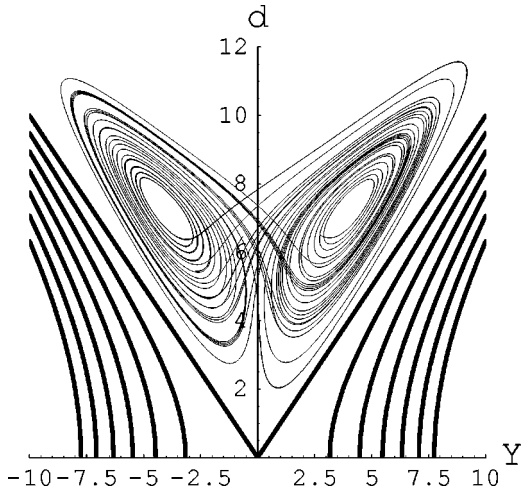

FIG. 9. Semipermeable surfaces (15) in case H ($d = \sqrt{-A_{1+}x^2 - (A_{1+}-1)z^2}$ with $A_{1+} < 0$) and chaotic attractor of system (2) with $\nu_1 = 1$, $\nu_2 = 4$, $\nu_3 = 1$, and $h = 6$.

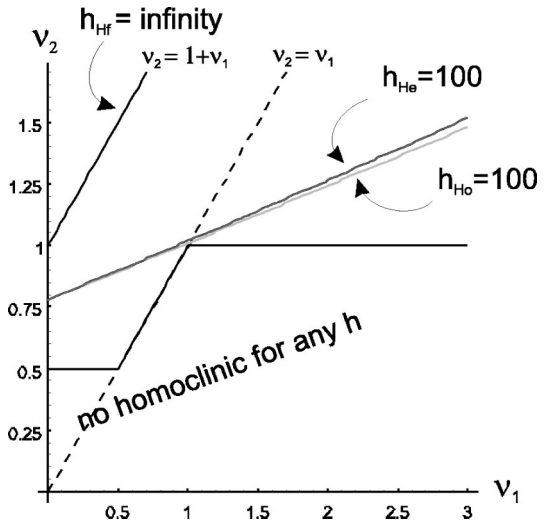

FIG. 10. Elements of the bifurcation diagram for system (2). Note that there is chaotic motion possible under the line $\nu_2=\nu_1+1$, which means that the system can be chaotic for some h even if the equilibrium points remain stable for all h. The curves $h_{\rm ho}=100$ and $h_{\rm he}=100$ were obtained numerically by a continuation method using MATHEMATICA.

the amplitudes of the three waves will not become chaotic for any value of the pump h. Above this region in the plane (ν_1,ν_2), we have to rely on numerical integration to draw a frontier $h_{\rm he}=+\infty$ (which seems to be a line) between two regions: in the lower region [which contains our exact region (20)] the instability in the plasma will never lead to chaotic behavior as in the upper region where there will be a value of the pump $h=h_{\rm he}$ for which the amplitudes of the waves will have a chaotic behavior.

IV. BOUNDING THE LYAPUNOV DIMENSION

Let us consider now the three Lyapunov exponents along the attractor: $\mu_1>0\geqslant\mu_2>\mu_3$. Thanks to numerical integration, we know that $\mu_1+\mu_2>0$, hence the Kaplan-Yorke formula for the Lyapunov dimension reads

$$D_L=2+\frac{\mu_1+\mu_2}{-\mu_3}. \tag{21}$$

Using the relation $\mu_1+\mu_2+\mu_3=-(\nu_1+\nu_2+\nu_3)$, we can write D_L as

$$D_L=2+\frac{\mu_1+\mu_2}{\mu_1+\mu_2+\nu_1+\nu_2+\nu_3}. \tag{22}$$

An upper bound of the (positive) sum of the first two Lyapunov exponents may be calculated by considering the maximum real part of the eigenvalues of the matrix $M(t)=(\boldsymbol{\nabla}\cdot\boldsymbol{F})\mathbb{I}-L(t)$, where $L(t)$ is the Jacobian matrix of the vector field and $\mathbb{I}$ is the 3D identity matrix [8]. For system (2), $\mu_1+\mu_2$ is bounded by the maximum real part of the eigenvalues of

$$M(t)=\begin{pmatrix} -\nu_2-\nu_3 & -h+z(t) & y(t) \\ -h-z(t) & -\nu_1-\nu_3 & -x(t) \\ -y(t) & -x(t) & -\nu_1-\nu_2 \end{pmatrix}. \tag{23}$$

At first sight, this trick seems to be of no help since one still needs numerical integration to evaluate the eigenvalues of the matrix $M(t)$. But if we consider that the values of $x(t)$, $y(t)$, and $z(t)$ on the chaotic attractor are bounded (thanks to the semipermeable surfaces), we may bound the eigenvalues of $M(t)$. The set of points Z, which lie above surface (4) with $b=0$ and $a=a_2$, inside surface (6) in case (AB), above surface (12) with $i=2$, and outside of the cone defined by surface (15) in case H, is a rather tight bound for the chaotic attractor:

$$(x,y,z)\in Z \quad \text{iff:}$$

$$z\geqslant\tfrac{1}{4}\,\frac{x^2+y^2}{h-\sqrt{(\nu_1-\frac{1}{2})(\nu_2-\frac{1}{2})}}, \tag{24}$$

$$h^2\geqslant x^2+(z-h)^2, \tag{25}$$

$$0\leqslant\nu_2(\nu_2-1)(x^2+y^2)[8hz-(x^2+y^2)] +2h^2[(1-2\nu_2)^2(x^2-y^2)+2z^2], \tag{26}$$

$$0\geqslant A_{1+}x^2+y^2+(A_{1+}-1)z^2. \tag{27}$$

Setting $\nu_1=1$, $\nu_2=4$, $\nu_3=1$, and $h=6$ and looking for the maximum real part of the eigenvalues of $M(t)$ for $(x,y,z)\in Z$ (for these values of parameters, $A_{1+}\simeq-0.6$), we found (unlike in [9]) that the largest real part is realized for $x=y\simeq5.82$, $z\simeq4.8$. Hence one finds that $\mu_1+\mu_2\lesssim4.31$ which yields $D_L\lesssim2.418$. Numerical integration yields $\mu_1\simeq0.39$, $\mu_2\simeq-0.001$, and $\mu_3\simeq-6.39$: $D_L\simeq2.061$.

V. CONCLUSION

In this work we have studied the dynamics of a 3D dissipative system which arises in the study of a parametric instability in a plasma.

We have established that the analytic information we have on the integrability of the system can be used to get information on the chaotic dynamics of this system. More specifically, we have shown that one can use the algebraic form of the integrals of motion (existing for specific parameters values) to bound the chaotic attractor in phase space and to bound the chaotic dynamics in the parameter space (by introducing analytic bounds to the homoclinic bifurcation curves). These results enable us to give information on the range of parameters for which the instability can lead to chaos.

We have also shown that one can use the geometric bounds introduced for the chaotic attractor to derive an upper bound for its Lyapunov dimension. We believe that this method can be used on any system with a constant divergence, regardless of its dimension.

ACKNOWLEDGMENT

The author would like to thank Y. Elskens for useful comments.

[1] T.F. Bell and H.D. Ngo, J. Geophys. Res. **93**, 2599 (1998).
[2] A.S. Pikovskii, M.I. Rabinovitch, and V.Y. Trakhtengerts, Sov. Phys. JETP **47**, 715 (1978).
[3] C. Sparrow, *The Lorenz Equations* (Springer-Verlag, Berlin, 1982).
[4] H. Giacomini, C. Repetto, and O. Zandron, J. Phys. A **24**, 4567 (1991).
[5] H. Giacomini and S. Neukirch, Phys. Lett. A **227**, 309 (1997).
[6] S. Neukirch and H. Giacomini, Phys. Rev. E **61**, 5098 (2000).
[7] T. McMillen, Nonlinear J. **1**, 1 (1998), available at http://www.math.arizona.edu/~goriely/nljournal/nljournal.html.
[8] A. Eden, C. Foias, and R. Temam, J. Dyn. Diff. Eqns. **3**, 133 (1991).
[9] C. Doering and J. Gibbon, Dyn. Stab. Syst. **10**, 225 (1995).